ORIGINAL ARTICLE
Iran J Allergy Asthma Immunol
August 2023; 22(5):440-451.
DOI:

MicroRNA-29a-3p Accelerates Inflammatory Damage in Neonatal Pneumonia Via Targeting Krüppel-like Factor 4

Xiao Juan Xu, Wei Liu, and ShiNa Liland

Department of Neonatal Ward, Yantai Yuhuangding Hospital, Yantai City, Shandong Province, China

Received: 7 February 2023; Received in revised form: 26 August 2023; Accepted: 26 August 2023

ABSTRACT

Neonatal pneumonia (NP) is a frequently occurring illness during the neonatal phase. The study investigated the molecular process and the role of microRNA (miR)-29a-3p in NP.

Peripheral blood was collected from NP patients and healthy newborns. Human lung fibroblasts cell line (WI-38) were treated with lipopolysaccharide (LPS)) to establish a cellular model for NP. Then, miR-29a-3p and Krüppel-like Factor 4 (KLF4) levels were detected by RT-qPCR or Western blot. The relationship between miR-29a-3p and KLF4 was confirmed by dual luciferase reporter gene assay. Cell survival was assessed using the CCK-8 assay, whereas the levels of interleukin-6, tumor necrosis factor-α, and IL-1β were quantified using ELISA. Additionally, apoptosis was evaluated through flow cytometry. Meanwhile, Bax and Bcl-2 were detected by RT-qPCR. Neonatal rats were administered LPS intraperitoneally (3 mg/kg) to induce NP, and pathological injury and inflammatory reaction were analyzed.

MiR-29a-3p was elevated but KLF4 was silenced in NP patient's serum, LPS-treated WI-38 cell line, and LPS-treated newborn rats. Silence of miR-29a-3p or elevation of KLF4 constrained cell proliferation with inflammation of LPS-treated WI-38 cell line. MiR-29a-3p immediately targeted KLF4. Additionally, silence of miR-29a-3p alleviated LPS-stimulated lung injury and inflammation in neonatal rats. The protective action of silenced miR-29a-3p in LPS-treated WI-38 cell line and newborn rats was turned around by silencing KLF4.

This study demonstrates originally that miR-29a-3p boosts inflammatory damage in NP via targeting KLF4, offering a basis for clinically diagnosing and treating NP.

Keywords: Krüppel-like factor 4; MicroRNA; Neonate; Pneumonia

INTRODUCTION

Neonatal pneumonia (NP) causes morbidity and mortality worldwide, killing 152,000 to 490,000 infantsunder one year of age each year,[1] mainly in developing countries in South Asia and sub-Saharan Africa.[2] NP is classified into neonatal aspiration pneumonia and neonatal infectious pneumonia from the etiology and it is caused by a viral or bacterial infection.[3] Pneumonia is not only infectious but also causes inflammation, thereby resulting in reduced oxygenation, shortness of breath and death [4] and is prone to

Corresponding Author: ShiNa Liland, MD;
Department of Neonatal Ward, Yantai Yuhuangding Hospital, Yantai City, Shandong Province, China. E-mail: lishina7722@outlook.com

*The first and second authors contributed equally to this study

complications like sepsis and respiratory distress syndrome.[5] Deaths from NP have declined due to antibiotic use,[6] while NP remains a considerable global health burden. Additionally, local signs of pulmonary infection in neonates are less than those in older children, so the diagnosis of NP is enormously challenging, and it is urgent to develop brand-new biomarkers for early diagnosis.[7]

MicroRNAs (miRNAs) can regulate genes after transcription and participate in a variety of biological processes.[8] Zhang Xiao et al,[9] discovered that hsa-miR-10a-3p, hsa-miR-1271-5p, hsa-miR-30b-3p, and hsa-miR-125b-5p exhibit increased levels. in pneumonia children. These microRNAs are involved in inflammation and immune responses, impacting pathways including NF-κB, mitogen-activated protein kinase, and T cell receptor signaling pathways. They hold promise as circulating biomarkers and therapeutic targets for managing pediatric pneumonia. miR-302e is downregulated in NP and miR-302e overexpression alleviates inflammation in NP via targeting the RelA/bromodomain-containing protein 4/NF-κB pathway.[10] miR-29a-3p, an extensively studied miRNA, has been discovered to exert a crucial action in multiple cancers like liver cancer,[11] endometrial cancer,[12] and gastric cancer.[13] Due to its high specificity and sensitivity, miR-29a-3p has been used as a novel biomarker in the diagnosis of COVID-19 to distinguish between acute and post-acute phases of the disease.[14] Nevertheless, its role in NP is unknown.

The research explored miR-29a-3p's action with molecular mechanisms in NP, offering a basis for the clinical diagnosis and treatment of NP.

MATERIALS AND METHODS

Clinical Samples

Serum samples were obtained from 40 NP patients and 40 healthy newborns in Yantai Yuhuangding Hospital. Neonatal venous blood was collected within 24 h after diagnosis. All samples were frozen in liquid nitrogen.

Cell Culture and Treatment

Human WI-38 cell line (CL) (China Center for Type Culture Collection, Wuhan, China) were cultured in DMEM (Gibco, USA). The medium covers 10% FBS (Gibco), 100 U/ mL penicillin (Beyotime, China) and 100 μg/ mL streptomycin (Beyotime). Replacement of the medium was implemented every day. To induce inflammatory injury, cells were treated with LPS at 10 μg/mL (Sigma-Aldrich) for 12 h.[15,16]

Cell Transfection

miR-29a-3p inhibitor/mimic, inhibitor/mimic NC, overexpression (oe)-Krüppel-like factor 4 (KLF4)/nontargeting control (NC) and si-KLF4/NC (all purchase was from GenePharma, Shanghai, China) were utilized to intervene in gene expression. When growing to 70%–80% confluence, WI-38 CL were transfected with the above-mentioned vectors (50 nM) using Lipofectamine 2000 reagent (Thermofisher).

CCK-8 Assay

Cells were seeded in Beyotime (Shanghai, China) 96-well plates at 5×10^3 cells per well. After LPS stimulation, 20 μL CCK-8 solution (Bioswamp, Wuhan, China) was cultivated for 1 h in each well. Determination of the absorbance at 450 nm was done with a microplate reader (Bio-Rad, Sunnyvale, CA).

Flow Cytometry

Analysis of cell apoptosis was implemented using PI and FITC combined with annexin V staining (Bioswamp). Cells were fixed on ice in 70% ethanol and stained with PI/FITC Annexin V in RNase A (Sigma), and incubated. Flow cytometry analysis was implemented on the FACScan (Beckman Coulter, USA). Data were analyzed by FlowJo (Tree Star, USA).

Experimental Animals

Newborn Sprague-Dawley rats (3-8 days of age, 8-14 g in weight) were purchased (Shanghai Experimental Animal Center) and kept under specific pathogen free (SPF) conditions with 12 h light/dark cycle. Anesthesia of neonatal rats was done with ether and then intraperitoneal injection with LPS at 3 mg/kg was performed (Sigma-Aldrich). After LPS injection, miR-29a-3p antagomir, antagomir NC, or miR-29a-3p antagomir + sh-KLF4/NC were given by intraperitoneal injection at 30 mg/kg (for 3 consecutive days). Euthanasia of rats was implemented after collecting blood from the eyeballs, and lung tissue was collected and stored in liquid nitrogen.

ELISA

Quantification of inflammatory cytokines in serum and WI-38 cell culture supernatant was implemented using ELISA kits in line with the protocol of the

manufacturer. Then, measurement of the absorbance at 450 nm was performed on a microplate reader. The concentration of inflammatory cytokines was normalized and calculated.

Hematoxylin-eosin (HE) Staining

Lung tissues were fixed with 4% paraformaldehyde and paraffin-embedded to prepare 5 μm-thick sections for HE staining (Sigma). Observation and scoring of histopathology were performed under a light microscope equipped with 400 magnifications (Leica Microsystems, Wetzlar, Germany).

Lung Histopathological Scoring

Based on a previous study, [17] we evaluated the pathological injury of lung tissue in rats according to the following scoring criteria.

A. The area of parbronchial inflammation injury (site ratio). 0=complete trachea structure, no surrounding abnormalities; 1=less than 25% peribronchial inflammatory infiltration; 2=inflammatory cell infiltration of 25-75%; 3 = more than 75% area inflammation.

B. Changes in the number and structure of inflammatory cells around the bronchus. 0=no inflammatory cells or occasional lymphocytes; 1=mild edema of the bronchial ring with frequent discontinuity; 2= moderate edema, annular structure close to complete or crescent ring, equivalent to the thickness of 5 cells; 3=Increased lymphocyte infiltration, severe ring formation, thickness close to 5-10 cells.

C. Inflammatory exudation volume of alveolar cavity. 0=clear and complete alveolar structure, no inflammatory factors; 1=mild inflammatory cell infiltration, accounting for less than 25% of the alveolar closed space; 2=25% cavity closure.

D. 0=No abnormal capillary structure in the capillary infiltration range; 1=infiltration area less than 10%; 2=10-50% of infiltrated area; 3=Area of tissue infiltration around pulmonary vessels increased to more than 50%.

Substantial pneumonia: 0=no substantial pathological changes; 1=pneumonia with mild consolidation or spotty parenchymal infiltration; 2=severe parenchymal lung disease with extensive infiltration with speckle enlargement or fusion.

The histopathological score (0- 26 points) was calculated as A+3 × (B + C) + D + E.

TUNEL Staining

After routine dewaxing and dehydration of paraffin sections, cell apoptosis was detected using a TUNEL kit (Nanjing Keygen Biotech Co., Ltd., Nanjing, China). Then, the nuclei were stained with 4, 6-diamidine-2-phenylindole (Beyotime, China) and observed under a fluorescence microscope (Nikon, Tokyo, Japan).[18]

RT-qPCR

Total RNA from serum, lung tissues or cells was collected using Trizol (Sigma). Total RNA (5 μg) was prepared into cDNA with a reverse transcription kit (Takara). Quantitative analysis was performed using SYBR Green Real-time PCR Master Mix reagent (Toyobo, Osaka, Osaka) on the ABI PRISM 7000 Sequence Detection system (ABI/Perkin Elmer, CA, USA) on the grounds of the standard protocol. PCR included 5 min at 95°C and 40 cycles of 30 s at 95°C, 30 s at 60°C, and 30 s at 72°C. GAPDH was the loading control for messenger RNA (mRNA), and U6 was that for miRNA. Relative expression was calculated via the $2^{-\Delta\Delta Ct}$ method. Primer sequences were manifested in Supplementary Table.

Western Blot

Extraction of total protein was implemented with RIPA lysis buffer (Sigma) plus protease with phosphatase inhibitors (Wolsen, China). Total protein (20 μg) was separated via 10% SDS-PAGE, electroblotted onto PVDF membrane (Millipore, USA), blocked with 5% skim milk, incubated with primary antibodies KLF4 (1: 1000, 4038, Cell Signaling Technology) and GAPDH (1: 1000, AB8245, Abcam, UK), re-incubated with horseradish peroxidase-conjugated secondary antibody (1: 1000, Cell Signaling Technolog, USA), and detected by a chemiluminescence detection kit (Millipore, USA).

Luciferase Activity Assay

The KLF4 3' untranslated region (UTR) fragment covering the wild-type (WT) or mutant-type (MUT) binding sites of miR-29a-3p was inserted into the psichecK-2 vector (Promega, Madison, WI). Subsequently, co-transfection with the luciferase reporter vector and miR-29a-3p mimic was performed on WI-38 CL using Lipofectamine 2000. After 24 h, analysis of luciferase activity was implemented via the luciferase reporting analysis system.

Data Analysis

Analysis of the whole data was performed using SPSS 21.0 statistical software. Measurement data were manifested as mean±standard deviation (SD). The two-group comparison of measurement data subjected to normal distribution was implemented with independent sample t test. Multiple-group comparisons were implemented with one-way analysis of variance (ANOVA) and Tukey's post hoc analysis. $p<0.05$ was accepted as indicative of distinct differences.

RESULTS

miR-29a-3p is Elevated, while KLF4 is Silenced in the Serum of NP Patients

The serum of NP patients was analyzed to determine the level of miR-29a-3p. It was found that miR-29a-3p exhibited a significant increase in NP cases ($p<0.001$). (Figure 1A). Furthermore, KLF4 levels were assessed in NP patients, revealing a notable decrease in KLF4 expression within the NP group ($p<0.001$) (Figure 1B). In addition to this, inflammation showed significant hyperactivation in NP patients ($p<0.001$) (Figure 1C-E). These results provide insight into the potential connection between miR-29a-3p, KLF4, and the inflammatory damage observed in NP.

Reducing miR-29a-3p Alleviates Inflammatory Damage in NP In vitro

WI-38 fibroblasts were treated with LPS to stimulate inflammatory injury. Detection of miR-29a-3p was performed, showing that miR-29a-3p was elevated in LPS-damaged WI-38 CL ($p=0.001$) (Figure 2A). Then, transfection was performed, showing that the miR-29a-3p inhibitor suppressed miR-29a-3p expression successfully ($p=0.001$) (Figure 2B). WI-38 cell viability was constrained after LPS treatment ($p=0.001$). Nevertheless, cell viability was strengthened after miR-29a-3p inhibitor intervention ($p=0.001$) (Figure 2C). Cell apoptosis was elevated after LPS treatment ($p<0.001$), and silence of miR-29a-3p was available to constrain cell apoptosis ($p<0.001$) (Figure 2D). Anti-apoptotic protein Bcl-2 was decreased ($p=0.001$) and pro-apoptotic protein Bax was increased ($p=0.001$) in LPS-damaged WI-38 CL, while Bcl-2 was increased ($p=0.003$) and Bax was decreased ($p=0.001$) after down-regulating miR-29a-3p (Figure 2E-F). miR-29a-3p inhibitor constrained LPS-stimulated inflammation in WI-38 CL ($p<0.001$) (Figure 2G-I). In general, suppressing miR-29a-3p protected LPS-damaged WI-38 CL from inflammatory damage.

miR-29a-3p Regulates KLF4 Expression

miR-29a-3p's immediate target was initially determined. As presented in Figure 3A, KLF4 is a potential target of miR-29a-3p predicted by starBase. It was further verified that KLF4 was the direct target of miR-29a-3p in WI-38 CL. As manifested in Figure 3B, the relative luciferase activity was distinctly suppressed after co-transfecting miR-29a-3p mimic with KLF4-WT. These results revealed that KLF4 was miR-29a-3p's direct target. Additionally, the association between miR-29a-3p and KLF4 was detected in LPS-introduced WI-38 CL. RT-qPCR and Western Blot results showed that down-regulating miR-29a-3p promoted KLF4 expression at mRNA ($p=0.002$) and protein levels ($p=0.004$) (Figure 3C). Additionally, miR-29a-3p level was reversely correlated with KLF4 in the serum of NP patients ($r = -0.600$, $p<0.001$) Figure 3D). In short, miR-29a-3p might mediate inflammatory injury via negatively modulating KLF4.

Inhibition of KLF4 Compensates the Impact of Reduced miR-29a-3p on Inflammatory Damage in NP In vitro

To figure out the impacts of KLF4 on miR-29a-3p -mediated inflammatory damage in NP, measurement of KLF4 in LPS-treated WI-38 CL was implemented. As manifested in Figure 4A, KLF4 was reduced in LPS-damaged WI-38 CL ($p=0.001$). Then, transfection of oe-KLF4/NC, miR-29a-3p inhibitor + si-KLF4/NC was conducted in WI-38 CL, and the transfection was verified by RT-qPCR ($p=0.001$) and Western Blot ($P = 0.002$) (Figure 4B). Elevated KLF4 enhanced cell viability, and silencing KLF4 mitigated the impact of miR-29a-3p low expression on cell viability ($p=0.001$) (Figure 4C). Additionally, elevated KLF4 constrained cell apoptosis, while silenced KLF4 offset the inhibition of miR-29a-3p downregulation on apoptosis ($p=0.001$) (Figure 4D). After elevating KLF4, Bcl-2 was elevated ($p=0.001$) and Bax was reduced ($p=0.002$), while silence of KLF4 was available to turn around the impact of miR-29a-3p downregulation on Bax ($p=0.003$) and Bcl-2 ($p=0.002$) (Figure 4E-F). For inflammatory cytokines, elevated KLF4 restrained inflammation, while silence of KLF4 was available to turn around the suppression of miR-29a-3p on inflammation ($p<0.001$) (Figure 4G-I). To sum up, silence of KLF4 attenuated the protection of

downregulated miR-29a-3p against inflammatory injury in NP.

MiR-29a-3p Boosts LPS-stimulated Lung Injury and Inflammatory Response in Neonatal Rats Via Targeting KLF4

The miR-29a-3p/KLF4 axis was further evaluated in pneumonia in an LPS-stimulated lung injury rat model. miR-29a-3p was elevated but KLF4 was suppressed in LPS-induced neonatal rats (p=0.001) (Figure 5A). Then, intraperitoneal injection with miR-29a-3p antagomir, antagomir NC, miR-29a-3p antagomir + sh-KLF4/NC was conducted. The successful injection was verified (p=0.002) (Figure 5B). Lung injury was detected by HE staining and TUNEL staining. LPS-treated rats had telangiectasia in lung tissue, thickened alveolar septa and capillary wall, inflammatory infiltration in the lung interstitium, and increased apoptosis. After suppressing miR-29a-3p, lung injury was significantly alleviated, only a small number of inflammatory cells infiltrated alveoli, and cell apoptosis was reduced. However, the alleviating effects of down-regulating miR-29a-3p on lung injury and cell apoptosis were offset by silencing of KLF4 (p<0.001) (Figure 5C-D). Additionally, silencing miR-29a-3p eliminated LPS-stimulated inflammation in rat serum, but the inhibition of inflammation by miR-29a-3p antagomir was offset by sh-KLF4 (p<0.001) (Figure 5E-G).

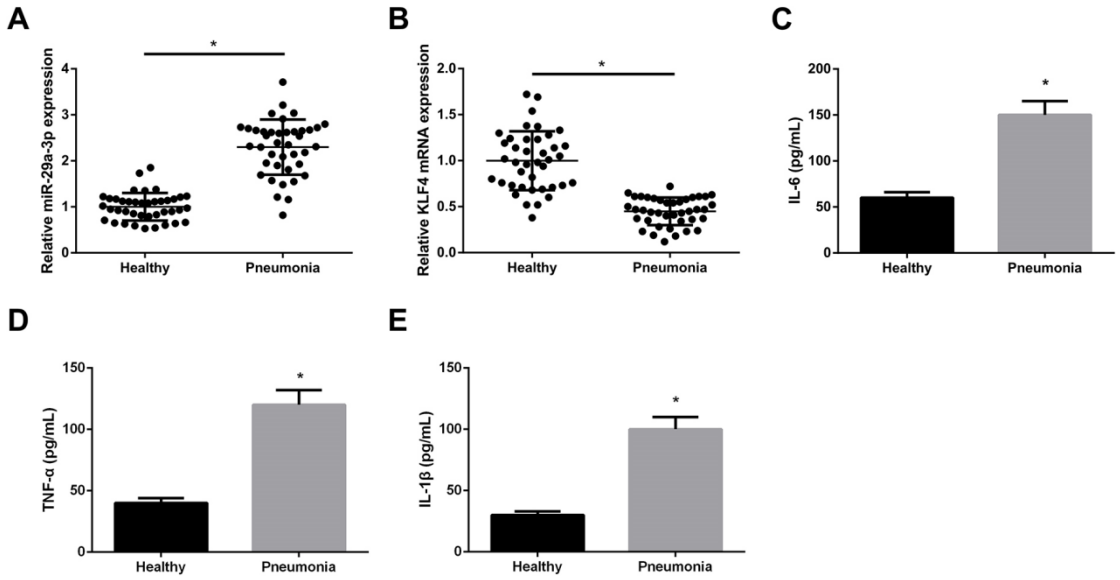

Figure 1. miR-29a-3p is elevated and KLF4 is silenced in serum of NP patients. A-B: RT-qPCR test of miR-29a-3p and KLF4 in NP patients' serum; C-E: ELISA detection of the contents of IL-6, TNF-α and IL-1β. Values are manifested in mean±SD (N=3). Independent sample t test was used for comparison between two groups, and one-way ANOVA and Tukey post hoc test were used for comparison between multiple groups. Comparisons have been made between the experimental groups and the control, *p<0.05.

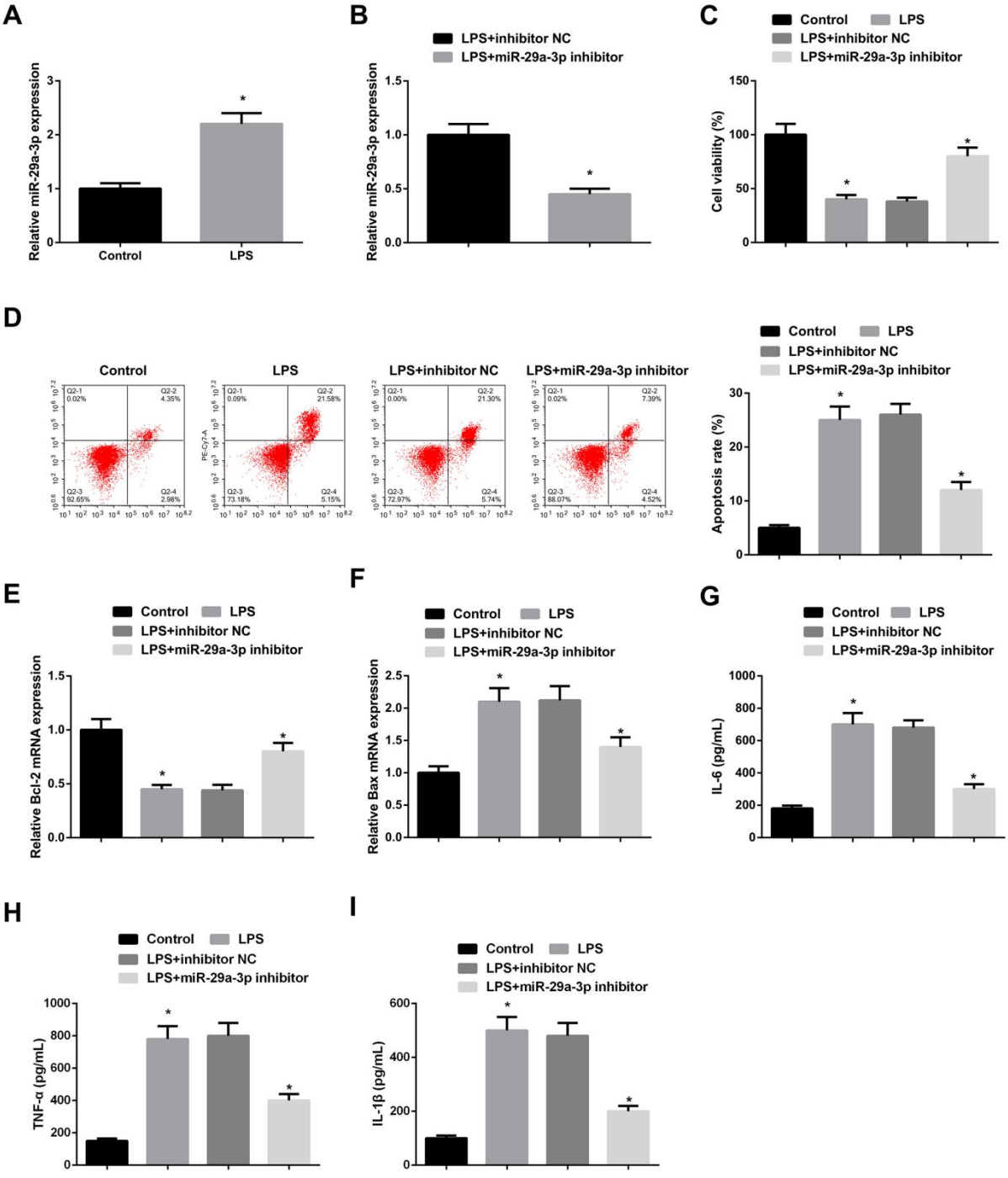

Figure 2. Silencing miR-29a-3p is available to alleviate inflammatory damage in NP in vitro. A: RT-qPCR test of miR-29a-3p in LPS-damaged WI-38 CL; B: RT-qPCR validation of successful transfection; C: CCK-8 test of cell viability; D: Flow cytometry examination of cell apoptosis; E-F: RT-qPCR test of mRNA of apoptosis-associated proteins (Bax and Bcl-2); G-I: ELISA examination of the contents of IL-6, TNF-α and IL-1β. Values are manifested in mean±SD (N=3). Independent sample t test was used for comparison between two groups, and one-way ANOVA and Tukey post hoc test were used for comparison between multiple groups. Comparisons have been made between the experimental groups and the control, *p<0.05.

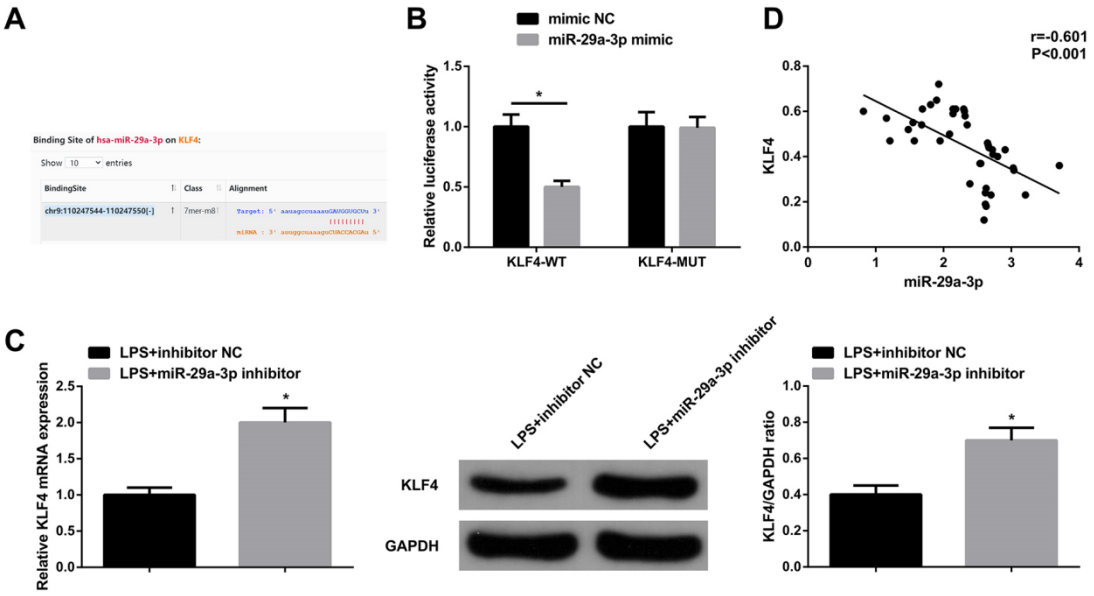

Figure 3. KLF4 is a target of miR-29a-3p

A: Starbase database found the targeted binding sites of miR-29a-3p with KLF4; B: The luciferase activity assay verification results; C: RT-qPCR and Western Blot examination of KLF4; D: Correlation analysis of miR-29a-3p with KLF4 in clinical samples; Values are manifested in mean±SD (N=3). Independent sample t test was used for comparison between two groups, and one-way ANOVA and Tukey post hoc test were used for comparison between multiple groups. Comparisons have been made between the experimental groups and the control, *p<0.05

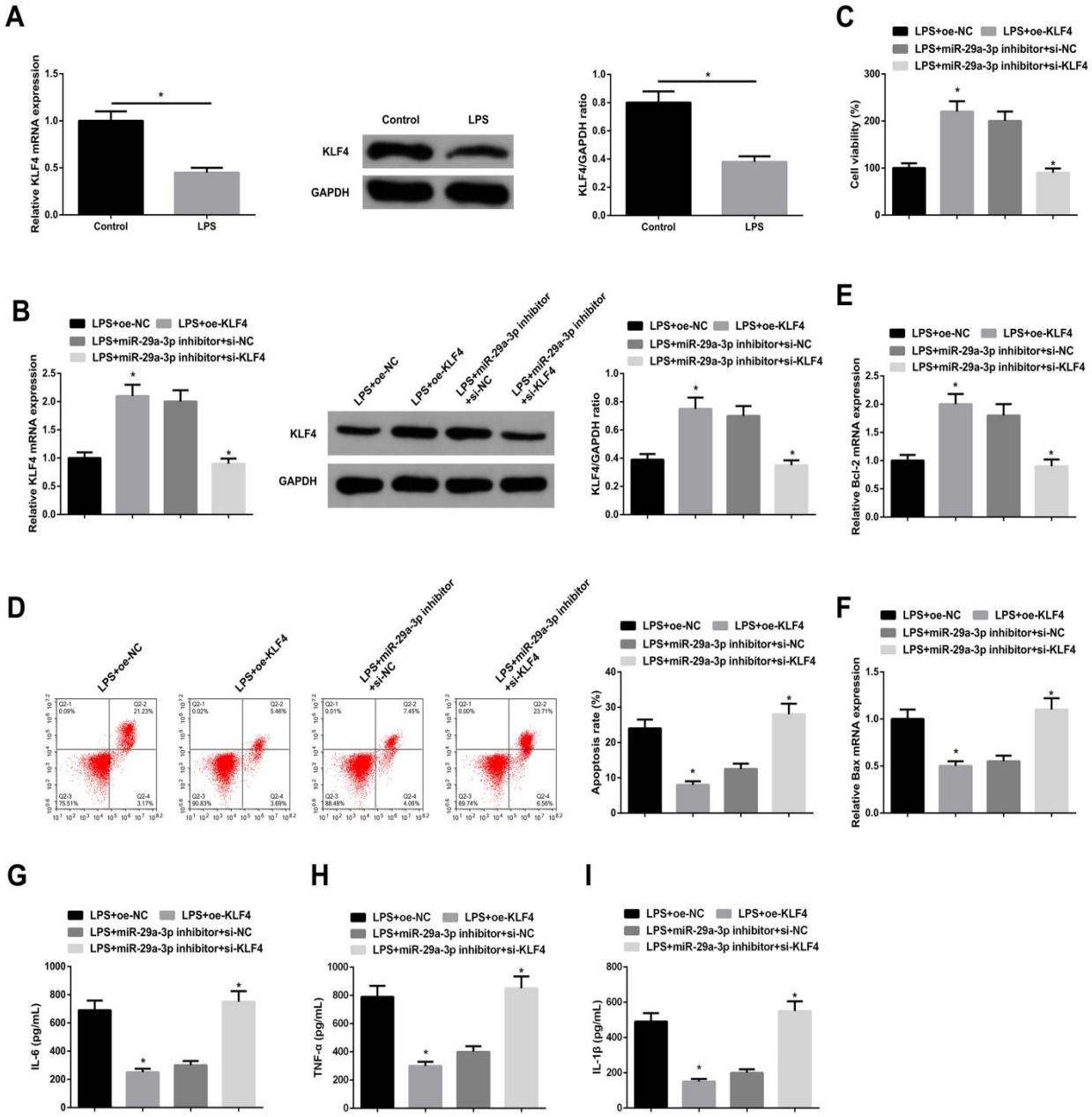

Figure 4. Silence of KLF4 offsets the impacts of silenced miR-29a-3p on inflammatory injury of NP in *vitro*

A: Test of KLF4 in LPS-damaged WI-38 CL; B: Validation of the successful transfection; C: CCK-8 examination of cell viability; D: Flow cytometry examination of cell apoptosis; E-F: RT-qPCR test of mRNA of apoptosis-associated proteins (Bax and Bcl-2); G-I: ELISA test of the contents of IL-6, TNF-α and IL-1β. Values are manifested in mean ± SD (N = 3). Independent sample t test was used for comparison between two groups, and one-way ANOVA and Tukey post hoc test were used for comparison between multiple groups. Comparisons have been made between the experimental groups and the control, *$p < 0.05$.

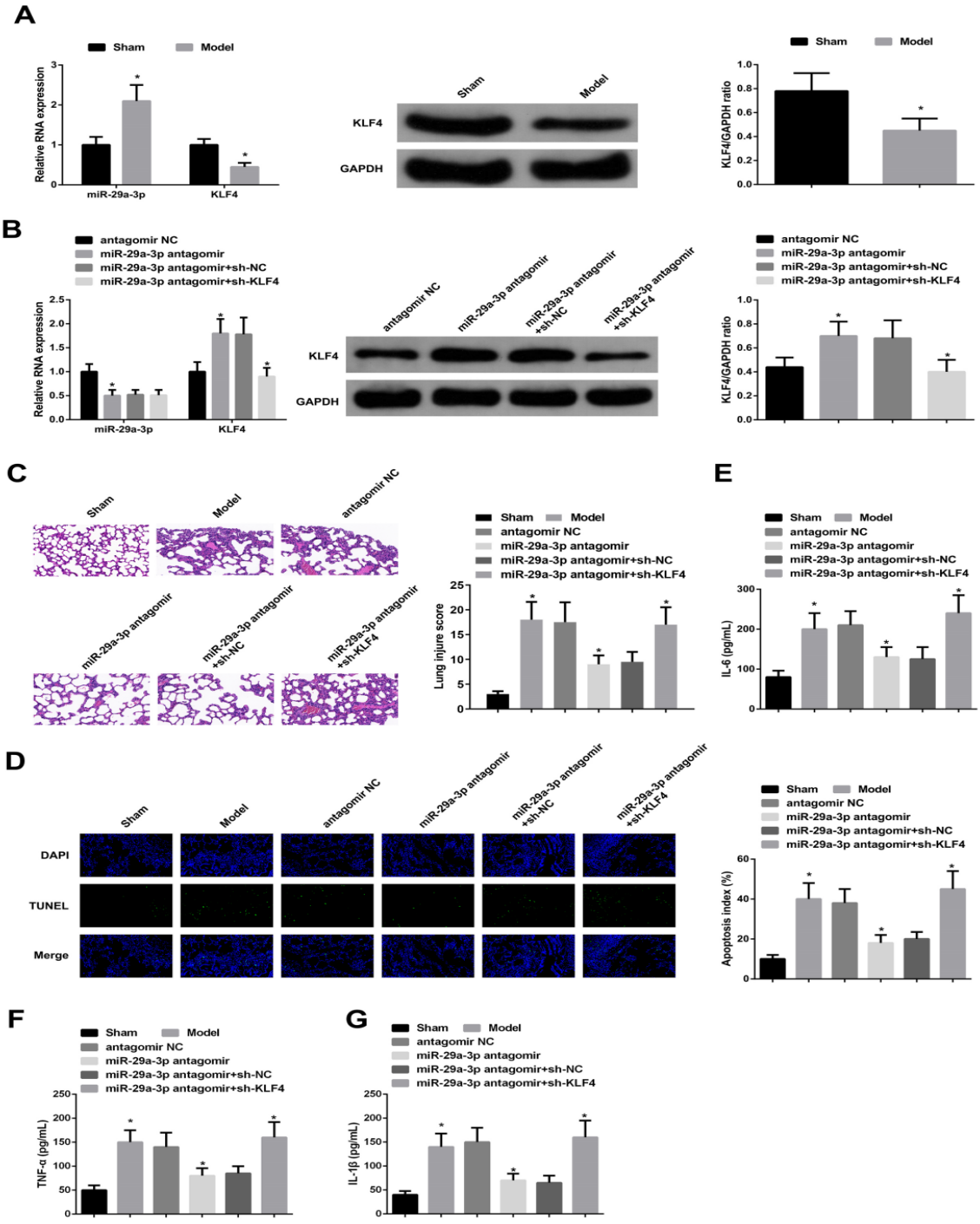

Figure 5. MiR-29a-3p boosts LPS-stimulated lung injury and inflammatory response in neonatal rats via targeting KLF4
A: Detection of miR-29a-3p with KLF4 in LPS-stimulated neonatal rats; B: Validation of successful injection; C: HE staining assessment of lung injury score in rats; D: TUNEL staining evaluation of apoptosis index in rats; E-G: ELISA examination of the contents of IL-6, TNF-α and IL-1β. Values are manifested in mean±SD (N=3). Independent sample t test was used for comparison between two groups, and one-way ANOVA and Tukey post hoc test were used for comparison between multiple groups. Comparisons have been made between the experimental groups and the control, *p<0.05.

DISCUSSION

NP is still an extremely common infectious disease in newborns, with a high mortality rate, which seriously endangers the life and health of children.[19] NP has a feature of over-release of inflammatory cytokines, leading to innate and acquired immunity activation.[20] As all know, LPS is available to trigger inflammatory damage in heterogeneous cells.[21] In this study, LPS was adopted to establish a cell model. As mentioned above,[22] it was observed that LPS constrained WI-38 cell proliferation and stimulated inflammation. These results manifested that LPS successfully led to WI-38 cell inflammatory injury. Through further studies, it was discovered that LPS treatment altered miR-29a-3p expression, while suppressing miR-29a-3p protected LPS-damaged WI-38 CL from inflammatory damage. Additionally, it was discovered that miR-29a-3p negatively mediated KLF4. Ultimately, in *in vitro* animal experiments, miR-29a-3p accelerated LPS-stimulated lung injury and inflammatory response in neonatal rats via targeting KLF4. The results manifested that miR-24 may become a prospective therapeutic target for NP.

LPS, a crucial constituent in Gram-negative bacteria's cell wall, is available to induce immune cells to secrete inflammatory factors to induce an inflammatory response.[23] LPS is broadly adopted to construct animal models of infectious injury. In this research, it was discovered that inflammation was augmented after LPS treatment, testifying that the experimental model was successful.

Aberrant miRNA is associated with the physiological and pathological processes of inflammatory diseases. For instance, miR-3941 controls LPS-stimulated acute pneumonia in A549 cells via targeting insulin-like growth factor-II.[24] MiR-20a promotes inflammation in pediatric pneumonia through NF-κB signaling.[25] miR-29a-3p is elevated in bronchopulmonary dysplasia mice, while elevated miR-29a-3p boosts inflammation and aggravates lung injury in bronchopulmonary dysplasia mice.[26] MiR-29a-3p is silenced in rats' myocardial tissue with severe acute pancreatitis and can be transmitted by extracellular vesicles from mesenchymal stem cells to suppress the induction of inflammatory markers to ameliorate cardiac function in myocardial injury.[27] Additionally, aberrant miR-29a-3p has been discovered in inflammation caused by myocardial ischemia-reperfusion injury,[28] hypoxic-ischemic brain injury,[29] Hashimoto's thyroiditis,[30] and adult Steele's disease.[31] In this research, miR-29a-3p level was elevated in NP patients, which was consistent with the foregoing result.[32] Silencing miR-29a-3p strengthened cell viability and suppressed inflammation in LPS-damaged WI-38 CL. Also, miR-29a-3p upregulation was also measured in LPS-stimulated lung injury rats, and silence of miR-29a-3p reduced LPS-stimulated lung injury, apoptosis, and inflammation. These results elaborated that miR-29a-3p exerted a crucial role in pneumonia-triggered inflammatory damage. Nevertheless, a foregoing study illuminated that miR-429 boosted inflammatory damage in NP via targeting KLF4.[33] In this research, the miR-29a-3p mediated inflammatory damage in NP via targeting KLF4.

KLF4 is a zinc-coated DNA-binding transcription factor that is involved in multiple tumors and acts as a tumor suppressor or oncogene in different tissues.[34] KLF4 was discovered to participate in inflammatory damage in NP.[33] Additionally, several studies have testified that KLF4 exerts a crucial action in pneumonia. For instance, KLF4 in phagocytes modulates the early inflammatory response and disease severity of pneumococcal pneumonia.[35] KLF4 is associated with LPS-stimulated apoptosis and inflammation in WI-38 CL.[36] In this study, it was found that KLF4 levels were diminished in both NP patients and WI-38 CL treated with LPS. Increased KLF4 levels enhanced cell viability and suppressed inflammation, whereas reduced KLF4 levels counteracted the impact of miR-29a-3p downregulation. These findings shed light on the role of miR-29a-3p in accelerating inflammatory damage in NP by targeting KLF4.

In brief, miR-29a-3p is elevated in NP patients. Silence of miR-29a-3p constrains inflammatory factors via targeting KLF4, thereby enhancing cell viability and alleviating inflammatory damage in NP. The study illuminates that miR-29a-3p might be a prospective curative target for NP.

STATEMENT OF ETHICS

All procedures performed in this study involving human participants were in accordance with the ethical standards of the institutional and/or national research committee and with the 1964 Helsinki Declaration and its later amendments or comparable ethical standards. All subjects was approved by the Yantai Yuhuangding Hospital (YT20210403).

FUNDING

This study does not have any funding for its execution.

CONFLICT OF INTEREST

The authors declare no conflicts of interest.

ACKNOWLEDGEMENTS

Not applicable.

REFERENCES

1. Global, regional, and national life expectancy, all-cause mortality, and cause-specific mortality for 249 causes of death, 1980-2015: a systematic analysis for the Global Burden of Disease Study 2015. Lancet (London, England) 2016, 388(10053):1459-1544.
2. Izadnegahdar R, Cohen A, Klugman K, Qazi S. Childhood pneumonia in developing countries. Lancet Respir Med. 2013;1(7):574-84.
3. Nissen M: Congenital and neonatal pneumonia. Paediatr Respir Rev. 2007; 8(3):195-203.
4. Peng X, Wu Y, Kong X, Chen Y, Tian Y, Li Q, et al. Streptococcus pneumoniaeNeonatal Pneumonia Induces an Aberrant Airway Smooth Muscle Phenotype and AHR in Mice Model. Biomed Res Int. 2019;2019(5):1948519.
5. Zaidi A, Ganatra H, Syed S, Cousens S, Lee A, Black R, et al. Effect of case management on neonatal mortality due to sepsis and pneumonia. BMC public health. 2011;S13.
6. Campbell H, El Arifeen S, Hazir T, O'Kelly J, Bryce J, Rudan I, et al. Measuring coverage in MNCH: challenges in monitoring the proportion of young children with pneumonia who receive antibiotic treatment. PLoS Med. 2013;10(5):e1001421.
7. Apisarnthanarak A, Holzmann-Pazgal G, Hamvas A, Olsen M, Fraser V. Ventilator-associated pneumonia in extremely preterm neonates in a neonatal intensive care unit: characteristics, risk factors, and outcomes. Pediatrics 2003, 112:1283-1289.
8. Abd-El-Fattah A, Sadik N, Shaker O, Aboulftouh M. Differential microRNAs expression in serum of patients with lung cancer, pulmonary tuberculosis, and pneumonia. Cell biochemistry and biophysics 2013, 67(3):875-884.
9. Zhang X, Huang F, Yang D, Peng T, Lu G. Identification of miRNA-mRNA Crosstalk in Respiratory Syncytial Virus- (RSV-) Associated Pediatric Pneumonia through Integrated miRNAome and Transcriptome Analysis. Med Inflamm;2020.2020:8919534.
10. Li S, Cui W, Song Q, Zhou Y, Li J. miRNA-302e attenuates inflammation in infantile pneumonia though the RelA/BRD4/NF-κB signaling pathway. Inte J Mol Med. 2019;44(1):47-56.
11. Zhang H, Wang Y, Ding H. COL4A1, negatively regulated by XPD and miR-29a-3p, promotes cell proliferation, migration, invasion and epithelial-mesenchymal transition in liver cancer cells. Clin Transl Oncol. 23(10):2078-89.
12. Geng A, Luo L, Ren F, Zhang L, Zhou H, Gao X. miR-29a-3p inhibits endometrial cancer cell proliferation, migration and invasion by targeting VEGFA/CD C42/PAK1. BMC cancer. 2021;21(1):843.
13. Qu F, Zhu B, Hu Y, Mao Q, Feng Y. LncRNA HOXA-AS3 promotes gastric cancer progression by regulating miR-29a-3p/LTβR and activating NF-κB signaling. Cancer Cell Int. 2021;21(1):118.
14. Donyavi T, Bokharaei-Salim F, Baghi H, Khanaliha K, Alaei Janat-Makan M, et al. Acute and post-acute phase of COVID-19: Analyzing expression patterns of miRNA-29a-3p, 146a-3p, 155-5p, and let-7b-3p in PBMC. Int Immunopharmacol 2021, 97:107641.
15. Zhao YJ, Chen YE, Zhang HJ, Gu X. LncRNA UCA1 remits LPS-engendered inflammatory damage through deactivation of miR-499b-5p/TLR4 axis. IUBMB Life. 2021;73(2):463-473.
16. Yu Y, Yang T, Ding Z, Cao Y. Circ_0026579 alleviates LPS-induced WI-38 cells inflammation injury in infantile pneumonia. Innate Immun. 2022;28(1):37-48.
17. Huang Z, Liu X, Wu X, Chen M, Yu W. MiR-146a alleviates lung injury caused by RSV infection in young rats by targeting TRAF-6 and regulating JNK/ERKMAPK signaling pathways. Sci Rep. 2022;12(1):3481.
18. Wu Y, Li J, Yuan R, Deng Z, Wu X. Bone marrow mesenchymal stem cell-derived exosomes alleviate hyperoxia-induced lung injury via the manipulation of microRNA-425. Arch Biochem Biophys. 2021;697(12):108712.
19. Liu J, Liu F, Liu Y, Wang H, Feng Z. Lung ultrasonography for the diagnosis of severe neonatal pneumonia. Chest. 2014;146(2):383-8.
20. Bouras M, Asehnoune K, Roquilly A. Contribution of Dendritic Cell Responses to Sepsis-Induced Immunosuppression and to Susceptibility to Secondary Pneumonia. Frontt Immunol. 2018;9:2590.
21. McKallip R, Ban H, Uchakina O. Treatment with the hyaluronic Acid synthesis inhibitor 4-methylumbelliferone

suppresses LPS-induced lung inflammation. Inflammation. 2015;38(3):1250-9.
22. Zhou Z, Zhu Y, Gao G, Zhang Y. Long noncoding RNA SNHG16 targets miR-146a-5p/CCL5 to regulate LPS-induced WI-38 cell apoptosis and inflammation in acute pneumonia. Life Sci. 2019;228(3)189-97.
23. Dagvadorj J, Shimada K, Chen S, Jones H, Tumurkhuu G, Zhang W, et al. Lipopolysaccharide Induces Alveolar Macrophage Necrosis via CD14 and the P2X7 Receptor Leading to Interleukin-1α Release. Immunity. 2015;42(4):640-53.
24. Fei S, Cao L, Pan L. microRNA-3941 targets IGF2 to control LPS-induced acute pneumonia in A549 cells. Mol Med Reports. 2018;17(3):4019-26.
25. Liu Z, Yu H, Guo Q. MicroRNA-20a promotes inflammation via the nuclear factor-κB signaling pathway in pediatric pneumonia. Mol Med Reports. 2018;17(1):612-7.
26. Zhong Q, Wang L, Qi Z, Cao J, Liang K, Zhang C, Duan J. Long Non-coding RNA TUG1 Modulates Expression of Elastin to Relieve Bronchopulmonary Dysplasia via Sponging miR-29a-3p. Front ped. 2020;8:573099.
27. Ren S, Pan L, Yang L, Niu Z, Wang L, Feng H, Yuan M. miR-29a-3p transferred by mesenchymal stem cells-derived extracellular vesicles protects against myocardial injury after severe acute pancreatitis. Life Sci. 2021;272:119189.
28. Tian R, Guan X, Qian H, Wang L, Shen Z, Fang L, Liu Z. Restoration of NRF2 attenuates myocardial ischemia reperfusion injury through mediating microRNA-29a-3p/CCNT2 axis. BioFactors (Oxford, England). 2021;47(3):414-26.
29. Huang W, Xiao F, Huang W, Wei Q, Li X. MicroRNA-29a-3p strengthens the effect of dexmedetomidine on improving neurologic damage in newborn rats with hypoxic-ischemic brain damage by inhibiting HDAC4. Brain research bulletin 2021, 167:71-79.
30. Tokić S, Štefanić M, Glavaš-Obrovac L, Kishore A, Navratilova Z, Petrek M. miR-29a-3p/T-bet Regulatory Circuit Is Altered in T Cells of Patients With Hashimoto's Thyroiditis. Front Endocrinol. 2018;9:264.
31. Hu Q, Gong W, Gu J, Geng G, Li T, Tian R, et al. Plasma microRNA Profiles as a Potential Biomarker in Differentiating Adult-Onset Still's Disease From Sepsis. Front Immunol. 2018;9:3099.
32. Keikha R, Hashemi-Shahri S, Jebali A. The relative expression of miR-31, miR-29, miR-126, and miR-17 and their mRNA targets in the serum of COVID-19 patients with different grades during hospitalization. Eur J Med Res. 2021;26(1):75.
33. Zhang L, Yan H, Wang H, Wang L, Bai B, Ma Y. MicroRNA (miR)-429 Promotes Inflammatory Injury by Targeting Kruppel-like Factor 4 (KLF4) in Neonatal Pneumonia. Curr Neurovasc Res. 2020;17(1):102-9.
34. Yang H, Park D, Ryu J, Park T. USP11 degrades KLF4 via its deubiquitinase activity in liver diseases. Journal o J Cell Mol Med. 2021;25(14):6976-87.
35. Herta T, Bhattacharyya A, Rosolowski M, Conrad C, Gurtner C, et al. Krueppel-Like Factor 4 Expression in Phagocytes Regulates Early Inflammatory Response and Disease Severity in Pneumococcal Pneumonia. Front Immunol. 2021;12:726135.
36. Wang Q, Zhang X, Chen D. circ_VMA21 protects WI-38 cells against LPS-induced apoptotic and inflammatory injury by acting on the miR-409-3p/KLF4 axis. Gen Physiol Biophys. 2021;40(4):275-87.